



Improving electrodialysis based water desalination using a sulfonated Diels-Alder poly(phenylene)



Timothy D. Largier^a, Donghui Wang^b, Joshua Mueller^a, Chris J. Cornelius^{a,*}

^a Department of Chemical and Biomolecular Engineering, University of Nebraska, Lincoln, NE, 68588, USA

^b Envonik, Birmingham, AL 36582, USA

ARTICLE INFO

Keywords:

Nernst Planck Equation
Nafion, Sulfonated polyphenylene, Ionomer
Ion and salt transport

ABSTRACT

Desalination performance using electrodialysis (ED), and electrochemical and state of water analysis is reported for the acid and sodium forms of a sulfonated Diels-Alder poly(phenylene)s (sPP) series. sPP ionomers had proton conductivities reaching 122 mS/cm with a water uptake of 105 wt%. At this composition, its film conductivity and water uptake in the sodium form decreased to 19 mS/cm and 42 wt%. Atomic force microscopy and x-ray scattering indicate that the rigid poly(phenylene) backbone results in a highly homogeneous intermediate phase containing large, disperse, and hydrophilic aggregates. Liquid transport experiments revealed that alcohol and sodium chloride diffusion is significantly lesser for the sPP series, which confirms differences in hydrophilic domain size and connectivity. In a working electrodialysis system, sPP (IEC=1.4 meq/g) desalinated 1.0 L of 0.1 wt% NaCl using 5.8 J/g or 5.8 kJ within 44 min. Commercial cation (PC-SK) and anion (PC-SA) exchange membranes designed for brackish water desalination required 8.4 J/g or 8.4 kJ and 79 min for the same volume and concentration. ED performance was adequately modeled by the Nernst-Planck equation, which is comprised of electroosmotic (migration) and diffusion contributions.

1. Introduction

Electrodialysis (ED) is a process by which ion-exchange membranes are alternately arranged in a direct current, typically used to demineralize, concentrate, or convert salt containing solutions [1]. An ED cell consists of a feed stream and brine stream, formed by semi-permeable anion and cation exchange membranes. During ED operation, ion-transfer is dominated by electroosmotic flux described as the migration of a charged species under the influence of an electric field. This migration phenomenon includes both the ionic solute and a shell of water molecules that accompany it, termed “electroosmotic drag.” Other contributions are those of ion diffusion and convection, the latter describing the bulk diffusion of solute due to solvent diffusion.

Although promising, ED suffers from economical limitations due to ion-exchange membrane (IEM) cost and short lifetimes caused by exposure to high-density electrical fields. Other desirable IEM properties include processability, good mechanical strength, low swelling, and high ion conductivity and selectivity. Therefore, it is imperative that a thorough understanding of ionomer properties is attained and optimized to ensure competitive system longevity and performance. Material research efforts have focused upon interrelationships among polymer chemistry, morphology, and ion conductivity/selectivity. A commercially available perfluor-

osulfonate ionomer, Nafion® by Dupont™, possesses high ionic conductivity and thermochemical stability [2], and it is considered the industrial standard in fuel cell and flow battery technology [3,4]. Nafion's electrochemical performance is attributed to a bicontinuous morphology, which is a property that increases ionic and molecular diffusion, and it is closely related to crossover inefficiencies [5]. This has inspired the development of alternative non-fluorinated ionomer chemistries such as poly(sulfone)s, poly(arylene)s, and poly(ether ketone)s [6–9].

Recently, a novel sulfonated Diels-Alder poly(phenylene) was reported that has good thermochemical stability, moderate swelling, and high proton conductivities [10,11]. The materials display great promise for use in various industrial applications, particularly in fuel cell and flow battery technologies [12,13]. In this work, an electrochemical and state of water analysis is performed for a series of sulfonated Diels-Alder poly(phenylene)s in the acid and sodium form. In addition, desalination data using electrodialysis is reported and analyzed.

2. Experimental

2.1. Materials

Poly(phenylene) was synthesized via Diels-Alder polymerization, as

* Corresponding author.

E-mail address: ccornelius2@unl.edu (C.J. Cornelius).

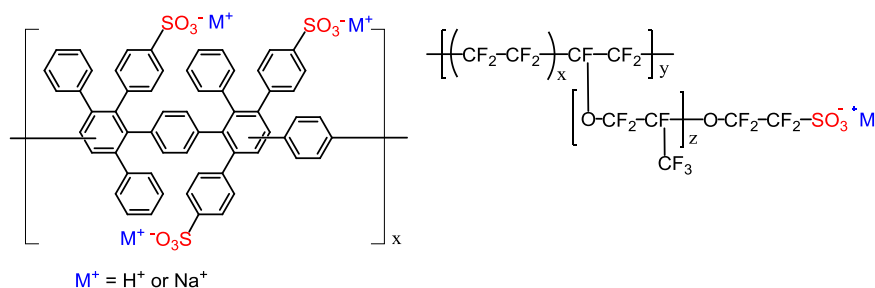


Fig. 1. Sulfonated poly(phenylene) (left) and Nafion® (right).

reported elsewhere by Cornelius and others [10,12,14–16]. Chlorosulfonic acid (97%), chloroform (>99.8%) and dimethylacetamide (>99%) were purchased from Acros Organics and used as received. Sulfuric acid 95.0–98.0 w/w%) and sodium hydroxide (>97.0%) were purchased from Fisher Scientific, and used as received. Dupont™ Nafion® 117 was purchased from The Fuel Cell Store©.

2.2. Poly(phenylene) sulfonation and solution-casting

The parent poly(phenylene) was functionalized by sulfonation using chlorosulfonic acid in chloroform (Fig. 1), as described elsewhere [10,11]. The procedure described is for a degree of sulfonation of 3. Poly(phenylene) (9.00 g, 11.8 mmol) was dissolved in 135 mL of methylene chloride and charged into a flame dried, mechanically stirred, reaction vessel. The vessel was put under an argon purge and the temperature lowered to -79°C (dry ice and acetone bath). A solution of chlorosulfonic acid (4.13 g, 35.48 mmol) in 5 mL of chloroform was added drop-wise over 5 min. After 30 min the reaction mixture was warmed to room temperature and the organic phase decanted to leave a black solid precipitate. 300 mL of 0.5 M NaOH solution was introduced into the reaction vessel, which, under stirring, was allowed to react overnight to ensure complete neutralization. The precipitate was then collected and washed with water to yield a tan solid.

Sulfonated poly(phenylene) membranes were cast from dimethylacetamide (5 wt% polymer). The solutions were filtered using a 45 μm PTFE syringe filter and poured onto a glass plate and placed within a vacuum oven. Films were allowed to form under vacuum for 24 h at 50°C , and then removed from the glass plate by submerging the plate in deionized water. The resulting polymer membranes were in the sodium salt (Na^+) form. Materials were converted into the acid form by heating preformed films in 1 M H_2SO_4 solutions at 90°C for 2 h. To ensure the removal of excess acid the materials were twice soaked in DI- H_2O at 90°C for one hour. The naming convention for sulfonated Diel-Alder poly(phenylene)s is “sPP” followed by the ion exchange capacity (IEC) in mequiv/g, determined by titration.

2.3. Material characterization

To confirm ionomer structure, FTIR was performed using a Nexus 670 ThermoNicolet FTIR with a deuterated triglycine sulfate (DTGS) detector and KBr beamsplitter. The equipment was operated with an aperture diameter of 8 mm with an approximate area of 0.50 cm^2 . For each sample, 50 scans were performed over a spectral range of $4000\text{--}400\text{ cm}^{-1}$.

A membrane's ion exchange capacity (IEC) was determined by converting it into the acid form by immersing it in a 0.5 M NaCl solution and allowed to neutralize. The solution was then titrated with a 0.02 M NaOH titrant to equivalence using a phenolphthalein indicator. The IEC is determined (mequiv/g) based upon the volume and molar concentration of the titrating NaOH solution (V_{NaOH} and M_{NaOH}), and membrane's initial mass in the acid form (W_{dry}) given by Eq. (1).

$$IEC = \frac{V_{NaOH}M_{NaOH}}{W_{dry}} \quad (1)$$

Membrane water uptake was determined gravimetrically. Thin films were soaked in deionized water at room temperature for 48 h. The membrane was then removed, quickly blot dried to remove surface water, and weighed to obtain a “wet mass” (m_{wet}). The membranes were dried under vacuum at 30°C for 24 h and then weighed to determine a “dry mass” (m_{dry}). The total water uptake (WU_{Total}) was determined using Eq. (2):

$$WU_{Total} = \left[\frac{m_{wet} - m_{dry}}{m_{dry}} \right] \times 100 \quad (2)$$

The average number of water molecules per sulfonic acid group is termed the hydration number (λ). This was calculated using Eq. (3).

$$\lambda = \frac{WU_{Total}}{IEC \times MW_{H_2O}} \quad (3)$$

The state of water was assessed using a TA instruments DSC Q20. Sulfonated samples were first soaked in DI- H_2O for 24 h, blot dried, and then weighed. In a typical run, under nitrogen, the temperature was increased from -50 to 75°C at a ramp rate of $10^\circ\text{C}/\text{min}$. The freezable water uptake ($WU_{Freezable}$) was determined by Eq. (4), where $Q_{f,w}$ is the heat of fusion for the freezable water endotherm peak (below 0°C), and ΔH_f is the heat of fusion for the ice-water transition (334 J/g).

$$WU_{Freezable} = \left(\frac{Q_{f,w}}{\Delta H_f} \right) WU_{Total} \quad (4)$$

Ion conductivity was determined using electrochemical impedance spectroscopy. The experiments were performed by applying a 10 mV signal and scanned over frequencies $100\text{--}100\text{ Hz}$. A Nyquist plot was generated, and the resistance was obtained where the non-real resistance was equal to zero. The ion conductivity was calculated using the equation $\sigma = L/(R A)$, where L is the length between the two sampling electrodes, R is the real resistance, and A is the membrane area available for proton conduction. For this study, experiments were performed in a temperature controlled water bath. Measurements were taken at 30°C , and ramped to 70°C .

In order to assess molecular diffusion through materials, a liquid diffusion apparatus was utilized. The apparatus included a water jacketed, membrane-separated, 20 mL PermeGear® diffusion cell. Both compartments were temperature controlled at 30°C , and vigorously stirred using submerged Teflon® magnetic stir bars. A one molar aqueous alcohol or salt solution was placed in one compartment, and pure deionized water (DI- H_2O) in the other. The DI- H_2O compartment had a sample stream that led to a Waters 410 Differential Refractometer, and then recirculated back to the compartment using a Waters 515 HPLC pump at $10\text{ mL}/\text{min}$. As alcohol diffused through the membrane the change in refractive index of the DI- H_2O compartment was monitored as a function of time. The RI signal was converted to an alcohol or salt concentration using a predetermined calibration

curve. On completion, data was collected in 10 °C increments from 30 to 70 °C. The Arrhenius equation was used to determine the activation energy of molecular diffusion by the slope of the natural log of diffusion versus inverse temperature.

Transmission small angle x-ray scattering (SAXS) was performed on a Rigaku SmartLab Diffractometer (Cu K α , $\lambda=154$ Å). Analysis was performed at 40 kV and 44 mA. The 2θ range for X-ray scattering was 0.2–1°, where θ is the incident angle covering a q range of 0.0142–0.712 nm $^{-1}$, and $q = 4\pi\sin\theta/\lambda$. Reflection wide angle x-ray scattering (WAXS) was performed with a 2θ range of 2–50°, where θ is the incident angle covering a q range of 0.14–3.45 Å $^{-1}$.

A Bruker Dimension Icon® Atomic Force Microscope (AFM) was used in tapping mode to image bulk film ionomer surface morphology. Sulfonated poly(phenylene) was scanned under the repulsive tip-sample interaction region, while the attractive interaction was used for Nafion 117. Silicon probes (TESPA-V2) were used with a cantilever spring constant ≈ 42 N/m, radius of curvature ≈ 8 nm, and resonance frequency ≈ 320 kHz.

To observe ionomer performance in desalination by electrodialysis, a PCCell BED1-4 unit was utilized. The system consisted of four electrolytic circuits, flow meters (10–100 L/h), and an electrodialysis cell (Fig. 2a). The performance of synthesized materials were compared to the commercial membranes provided by PCCellCorp, PC-SA (AEM) and PC-SK (CEM).

During ED operation the ion flux through a membrane can be related to the ion transport number (t_i), Faraday's constant (F), and current density (I) described by Eq. (5).

$$J_i = \frac{\bar{t}_i I}{F} \quad (5)$$

The ion transport number is described by where C_i is the dilute stream concentration, V is the dilute stream volume, and A is the effective area of the ion exchange membrane.

$$\bar{t}_i = \frac{FV}{IA} \left(\frac{dC_i}{dt} \right) \quad (6)$$

The flux was normalized by the number of membranes in the series. In order to determine flux contributions the Nernst-Planck equation was used. This equation describes the flux of ions influenced by an ionic concentration gradient and an electric field, and can be written as where z is the valence of the ionic species, R is the gas constant, T is the

temperature, D_i is the membrane ion diffusivity, C_i is the ion concentration within the membrane, and $d\phi/dx$ and dC_i/dx are the electric potential gradient and concentration gradient across the membrane.

$$J_i = -D_i \left[C_i \frac{zF}{RT} \frac{d\phi}{dx} + \frac{dC_i}{dx} \right] + J_w \sigma \quad (7)$$

Ion flux by bulk convection is described by the product of water flux (J_w) and a reflectivity constant (σ) that accounts for ion/solvent selectivity, however in this study it was considered negligible. In its steady state form, and using the concentration profile in Fig. 2b, the Nernst-Planck equation can be written where δ is the film thickness, and the subscripts l and m denote dilute stream and membrane properties. The salt concentration within the membrane is defined as the product of the polymers maximum ion content (mequiv/g) and density (g/mL). The applied potential across the membrane is estimated by dividing the applied current density (A/m 2) by the ionic conductivity (S/cm), normalized by the number of membranes in the series.

$$J_i = -D_i \left[C_m \frac{zF}{RT} \frac{\phi_m}{\delta} + \frac{C_d - C_m}{\delta} \right] \quad (8)$$

3. Results and discussion

3.1. Chemistry and morphology

In order to assess the structural changes in the polymer before and after functionalization infrared spectroscopy was performed. The stretching and bending vibrations of covalent bonds caused by radiation from the infrared region of the electromagnetic spectrum can confirm the presence of particular functional groups. In Fig. 3a the spectra for the parent poly(phenylene) (PP) and sPP1.4 is displayed. Phenyl carbon-carbon stretching typically occurs around 1500–1400 cm $^{-1}$ for phenylated molecules, and can be seen at 1490 cm $^{-1}$ and 1440 cm $^{-1}$. Carbon-hydrogen out of plane bending peaks are evident at 692 cm $^{-1}$ and 758 cm $^{-1}$. IR spectra for the sulfonated materials were normalized over the 1440 cm $^{-1}$ C-C phenyl peak. The data confirms the presence of sulfonic acid functional groups within the structure of the polymer. As expected there was little change in the stable aromatic carbon-carbon bonds located from 1400 to 1600 cm $^{-1}$.

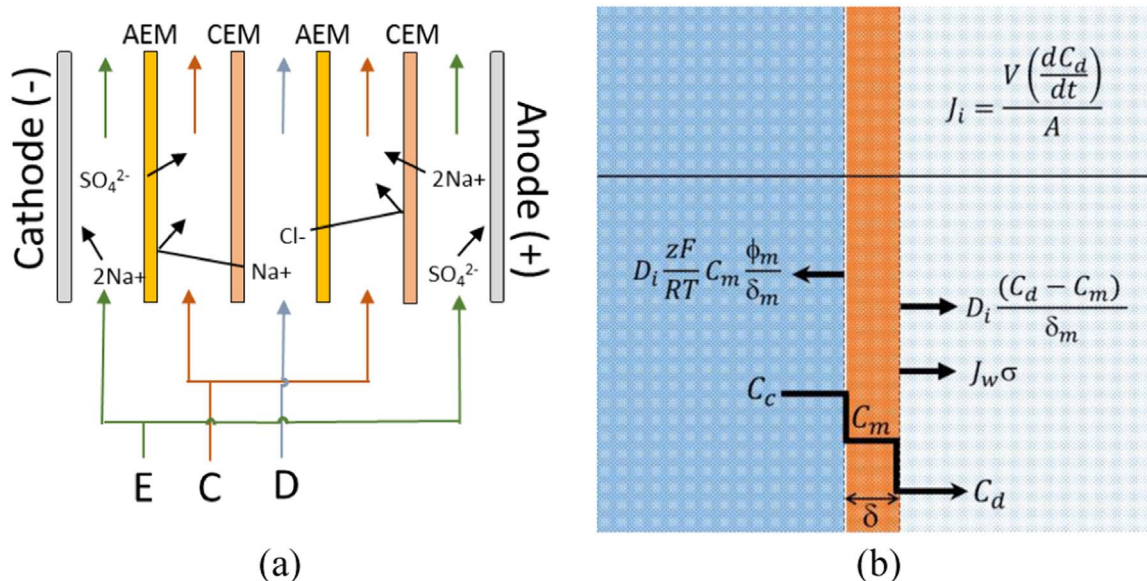


Fig. 2. (a) A schematic of the electrodialysis cell, where “E” denotes the electrode compartments, “C” the anodic and cathodic concentrate streams, and “D” the dilute stream. (b) The flux equation (top) and a simplified concentration profile used for the Nernst-Planck equation (bottom).

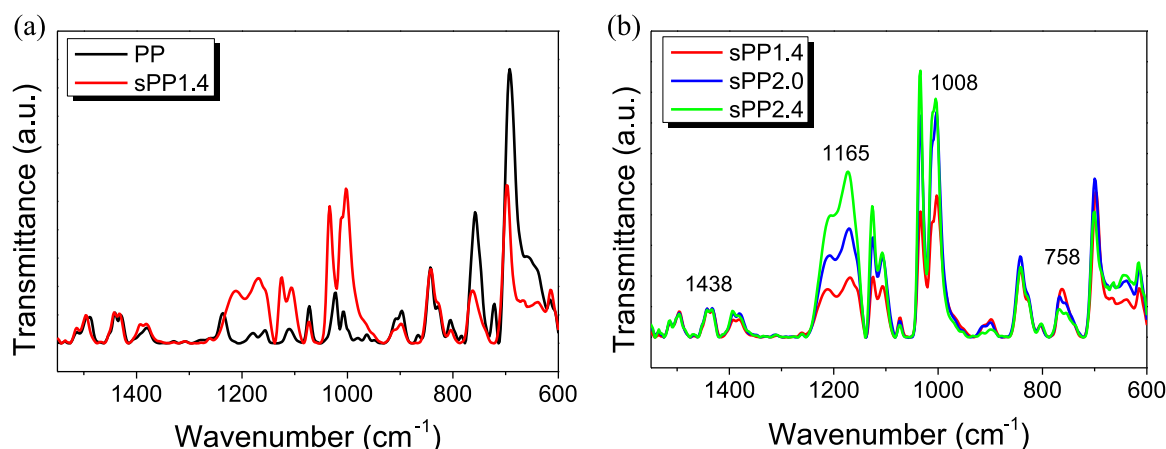


Fig. 3. FTIR spectra of the parent and acid form sulfonated Diels-Alder poly(phenylene)s.

The phenyl out of plane C-H peak at 758 cm^{-1} is diminished in the sulfonated polymer as hydrogen is lost during the sulfonation reaction. The $\text{S}^=\text{O}$ sulfonate group asymmetric and symmetric stretching can be seen at 1124 cm^{-1} and 1169 cm^{-1} , respectively, and an S-O stretch can be seen by a strong band at 1008 cm^{-1} . In Fig. 3b, peaks corresponding to sulfonic acid groups increase in intensity with increasing ion exchange capacity, while the phenyl C-H out of plane peaks (758 cm^{-1}) decrease in intensity confirming sulfonation on the pendant phenyl rings.

The phase images obtained by tapping mode atomic force microscopy for sPP and Nafion are displayed in Fig. 4. In this analysis, the hydrophilic regions of the sPP materials appear darker in color, while Nafion's are light in color (see experimental). The surface of the sulfonated poly(phenylene)s reveal a somewhat homogeneous ionic/intermediate phase, displaying a wide size distribution of hydrophilic regions from 0 to 25 nm. At an IEC of 2.4 meq/g sPP reveals a greater number of large domains. Nafion, with a low IEC of 0.95 meq/g, displays significant phase separation observed by small well-defined hydrophilic regions [17].

Grazing-incident wide angle x-ray diffraction patterns for all materials are shown in Fig. 5. Large peak breadths are the result of the amorphous nature of the materials [18–21]. In the diffraction patterns three peaks were identified and labelled d-1 through d-3 from the largest to smallest features, respectively. Peak d-2 (9.6 \AA) lies in a region that has been most commonly observed in atactic polystyrene, and has been referred to as the “polymerization peak” [22–24]. It has been determined that this region reflects inter chain packing [25]. The d-3 peak (5.2 \AA) has been termed the “amorphous halo”, and is commonly seen in polymer melts, glasses and rubbers. As seen in Fig. 5a, the increasing presence of the sulfonic acid group disrupts order associated with interchain packing. With increasing IEC there is an increase in relative intensity of the broad ionic d-1 peak, correlating to a d-spacing of roughly 24 \AA , similar in size to that of other amorphous sulfonate ionomers [26,27]. No significant peak shift is observed with increasing IEC. It is suspected that the ionic peak represents intra-particle scattering, whereby the aggregate size is limited by the low dielectric constant of the poly(phenylene) backbone and steric effects of the polymer chain. The increase in d-1 intensity with IEC would then indicate an increase in the number of scattering sites. Transmission SAXS was performed to contrast the ionic peak of the sPP materials to that of Nafion (Fig. 5b). Nafion displays an ionic peak correlating to a d-spacing of 35 \AA , greater than that for sPP. In addition Nafion's narrow peak breadth indicates a smaller aggregate size distribution. It is evident that sPP's rigid backbone inhibits ring reorientation, encouraging a wider distribution of smaller ionic aggregates.

3.2. Electrochemical properties and the state of water

A state of water analysis is imperative in the consideration of ion transport phenomena. Calorimetric studies on the freezing of water in ionomers has been extensively studied [28–31]. Three states have been identified, a bulk-like water that freezes at roughly $0\text{ }^{\circ}\text{C}$, loosely bound water that displays a broad heat of fusion at lower temperatures, and non-freezing strongly bound water. The width of the freezable endotherm peak can be correlated to molecules in a range of energetic states that cannot escape the binding environment near the ionic groups [30]. In this study all materials displayed little freezable bulk water that, at low IEC's, were distinct from the loosely bound endotherm peak. Obtaining heat of fusion values for freezable bulk water proved difficult due to peak size or overlap. These peaks were therefore evaluated together to calculate a “freezing/free water uptake”, and all remaining water is considered bound.

Fig. 6 displays the ion conductivity versus water uptake and the free/freezable water uptake for the acid (H^+) and sodium (Na^+) forms of sulfonated poly(phenylene) and Nafion 117. The acid form of sPP2.0 has a proton conductivity most similar to Nafion, however requires a significantly higher water content. These discrepancies in electrochemical properties are driven by the differences in morphology. It has been shown that Nafion exhibits ion aggregation and clustering causing the formation of polar micro-channels, allowing for effective water assisted ion diffusion [32,33]. Since the ionic domain clusters in sPP are smaller and more disperse a higher ion content is required to reach the percolation threshold, defined as a local concentration of ionic groups required to facilitate effective ion exchange via proton hopping or water-assisted ion diffusion [34,35]. A slight dilution effect in sPP2.4 is apparent, seen by an increase in water uptake yet disproportional increase in ion conductivity. Two other data sets have been included from literature; a sulfonated poly(ether ether ketone) (SPEEK) [36] and a sulfonate naphthalene dianhydride based polyimide (BAPS) [37]. It is concluded that sPP displays electrochemical performance competitive to these ionomer chemistries. Interestingly, despite vast differences in chemistry and morphology, Nafion 117 and sPP differ little in their relationship between proton exchange and free water (Fig. 6c). This highlights the importance of free/freezable water for the facilitation of ion exchange. In addition, the previously observed dilution effect in sPP2.4 is increased. The dilution effect therefore primarily presents itself as the inefficient use of free and loosely bound water.

The salt form of the materials display lower ion conductivities and water content than the acidic materials. In Table 2, it can be seen that sPP in the salt form displays a reduction in hydration number and increase in ratio of free water molecules, indicating a greater proportion of water in lower energetic states due to weaker ionic interactions (Table 1). Fig. 6d and e reveal that Nafion has a sodium ion

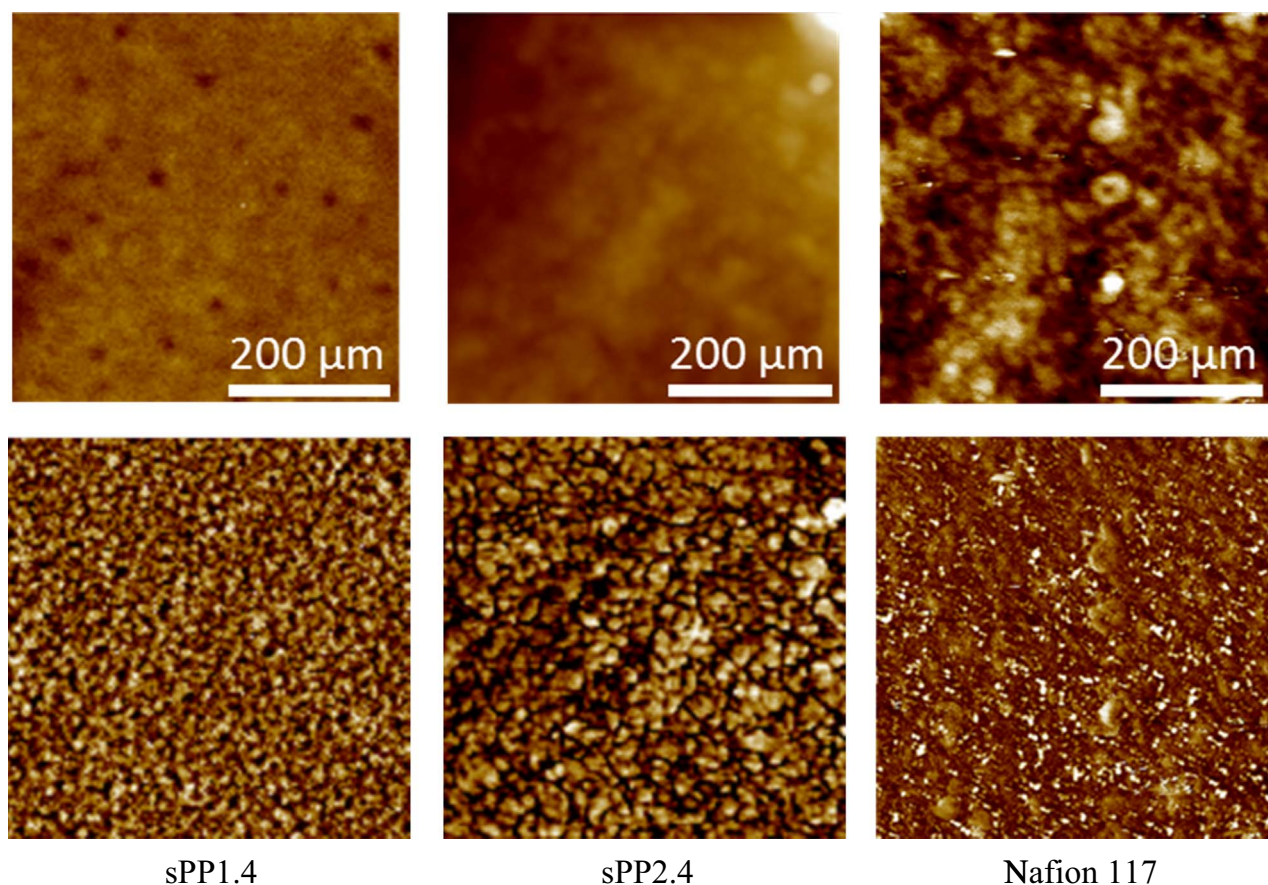


Fig. 4. AFM tapping mode surface images of hydrated Nafion 117 and sPP membranes. Height (top) and phase (bottom) images.

conductivity well above that of sPP2.0 attributed to the understood mechanism for the exchange of larger, less mobile, ions. While the acidic form of the material may allow for proton hopping (Grotthuss mechanism), the sodium form relies heavily on water assisted diffusion. The large micro-channels within Nafion's bicontinuous morphology therefore play a vital role in the facilitation of sodium ions through diffusion of water across the membrane. An Arrhenius relationship is observed for conductivity versus temperature (Fig. 6c,f) allowing for the calculation of an activation energy. The activation energy for ion

exchange decreases with increasing IEC and water uptake. The acid form of Nafion 117 displays an activation energy of (E_{a,H^+}) of 2.10 kcal/mol that is comparable to that of sPP2.0 and sPP2.4, which exhibit E_{a,H^+} of 2.09 and 1.89 kcal/mol, respectively. The salt form of Nafion 117 displays an E_{a,Na^+} of 12.64 kcal/mol, well below sPP2.4 of 13.61 kcal/mol. This is attributed to Nafion's bicontinuous morphology whereby sodium ion exchange increases with water permeability, a temperature dependent property that is integral for the facilitation of water assisted ion-diffusion [30–32].

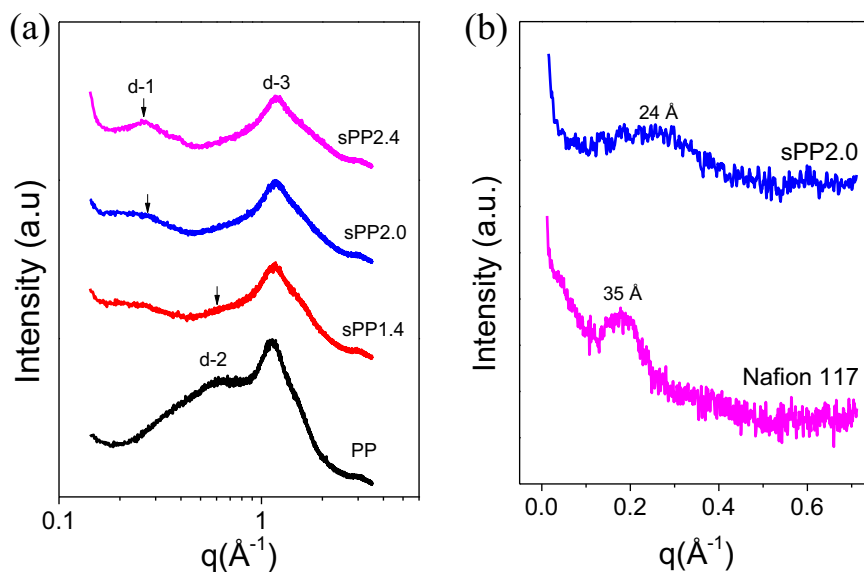


Fig. 5. (a) Reflection WAXS for the parent poly(phenylene) and sPP (Na^+). (b) Transmission SAXS for sPP2.0 (Cs^+) and Nafion 117 (Na^+).

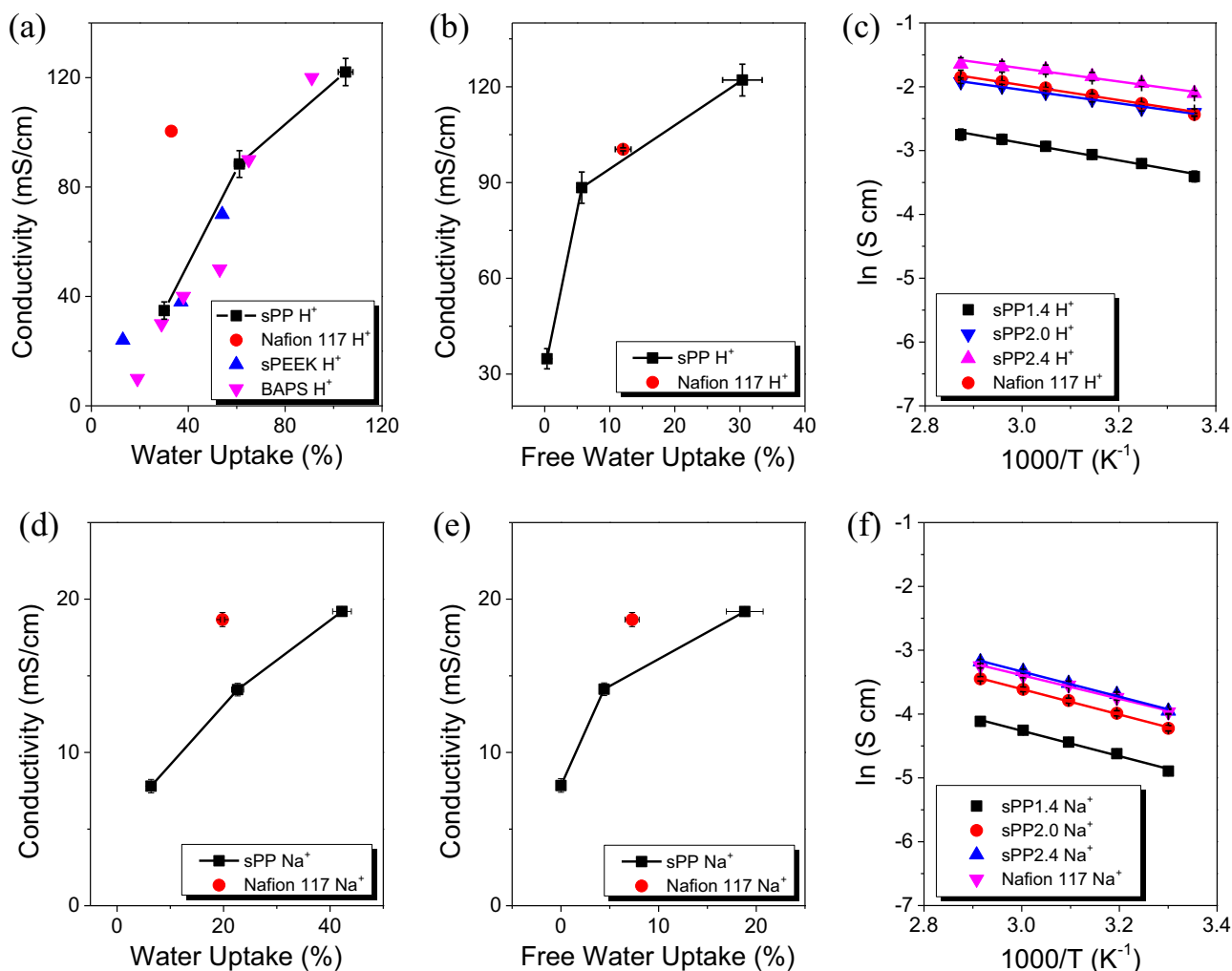


Fig. 6. The (a-c) acid and (d-f) salt form ion conductivity as a function of IEC, water content, and temperature.

Table 1

Ion conductivity, hydration number, total water uptake, free/freezable water uptake, and the heat of fusion for the loosely bound water peak for ionomers in the acid and sodium form.

	σ (mS/cm)	λ ($H_2O/SO_3^- M^+$)	WU _{Total} (%)	WU _{Free} (%)	f (free/bound)
sPP1.4H ⁺	34.8	12	30.1	0.4	0.0
sPP2.0H ⁺	88.4	17	61.1	5.7	0.1
sPP2.4H ⁺	122.1	24	105.0	30.4	0.4
Nafion 117H ⁺	100.4	20	33.0	12.1	0.6
sPP1.4 Na ⁺	7.8	3	6.4	0.0	0.0
sPP2.0 Na ⁺	14.1	6	22.6	4.4	0.2
sPP2.4 Na ⁺	19.2	10	42.2	18.8	0.8
Nafion 117 Na ⁺	18.7	12	19.8	7.3	0.6

Table 2

Methanol, ethanol, 2-propanol and sodium chloride permeability's (30 °C) and activation energy's for sulfonated poly(phenylene)s and Nafion 117.

	Permeability (10^8 cm ² /s)				Activation Energy (kcal/mol)			
	MeOH	EtOH	2-Prop.	NaCl	MeOH	EtOH	2-Prop.	NaCl
sPP1.4	57	27	12	2	3.3	6.0	9.1	4.9
sPP2.0	108	73	40	9	4.2	4.7	6.1	4.8
sPP2.4	184	134	89	30	4.2	4.7	5.5	3.6
Nafion 117	195	146	126	16	4.9	5.0	6.1	4.3

3.3. Liquid permeability

Table 2 displays alcohol and salt permeability data for the sulfonated poly(phenylene)s and Nafion 117. The liquid diffusion coefficients for sPP increase with ion content, consistent with the electrochemical and state of water analysis. An IEC increase from 2.0 to 2.4 meq/g results in a large increase in alcohol permeability, correlating to sPP2.4's greater free water content and observed dilution effect. Despite a significantly lower water content Nafion displays greater molecular diffusion. Alcohol diffusion studies serve to probe the size of the hydrophilic domains within the material, and the improved alcohol selectivity of sPP is consistent with the small and disperse ionic domains observed in the morphological analysis. Alcohol activation energies decrease with increasing IEC and increase with increasing alcohol size. As discussed, sPP2.0 displays lower alcohol permeability than Nafion 117, however it has higher activation energies. This

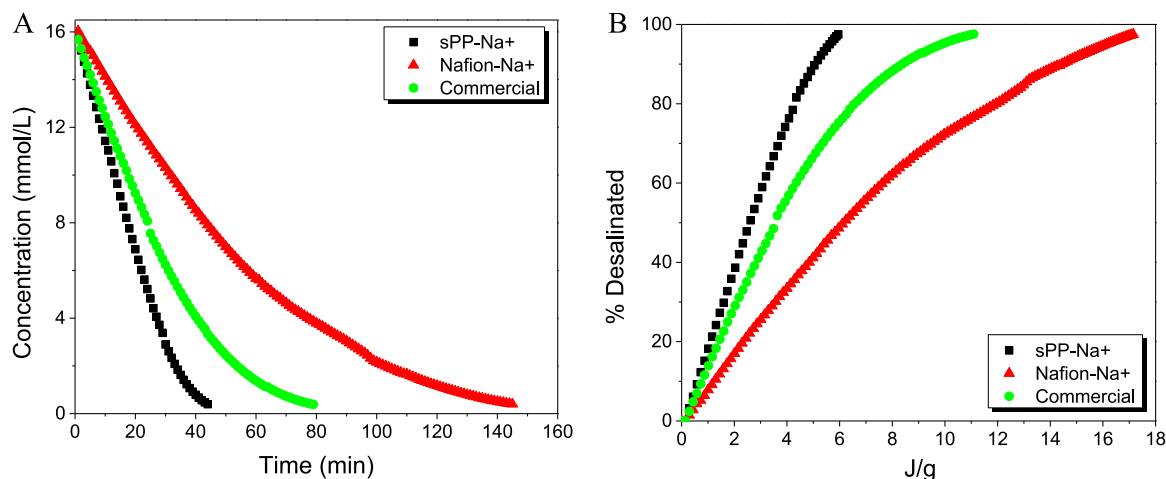


Fig. 7. A) Dilute stream concentration as a function time, and B) dilute stream %Desalinated as a function of total energy per gram of saline water.

Table 3

Parameters used to determine flux via the Nernst-Planck equation.

	IEC meq/g	σ_{Na^+} mS/cm	Salt Diff. $10^8 \text{ cm}^2/\text{s}$	Thickness μm
sPP1.4 Na ⁺	1.40	10.5	2.01	85
Nafion 117 Na ⁺	0.95	18.7	16.5	200

suggests improved domain connectivity in sPP induced by an increase in temperature-dependent swelling.

3.4. Electrodialysis performance

In this study the interrelationship between morphology, the state of water, and ion and molecular transport has been assessed. In agreement with a morphological characterization, Nafion is revealed to possess distinct ionic domains with good interconnectivity that result in a high ion conductivity and low water content. Conversely sPP possess a homogeneous morphology that requires greater exchange unit and water content to achieve the necessary free water to facilitate effective ion conductivity. However, liquid and sodium chloride diffusion studies reveal that the small, disperse, interconnected ionic domains substantially reduce molecular diffusion. sPP's electrochemical tune-ability and high molecular resistance are desirable ionomer

characteristics for electrodesalination applications. In Fig. 7 electrodesalination performance is displayed for sPP with an IEC of 1.4, Nafion 117; and commercial cation (PC-SK) and anion (PC-SA) exchange membranes designed for brackish water desalination. Despite excellent electrochemical properties and a low water uptake in the salt form, Nafion displays poor desalination performance. As revealed in the liquid permeability study, Nafion suffers from poor ion selectivity. This results in osmosis, or “back diffusion”, of salt increasing the desalination time and input energy needed to obtain ultra-pure water. sPP1.4 displays incredible performance with a desalination time of 44 min and an energy requirement of 5.8 kJ or 5.8 J/g, superior to that of the commercial standard PC-SA that demands 79 min and 8.4 kJ or 8.4 J/g of energy. It is therefore concluded that sulfonated Diels-Alder poly(phenylene)s, which exhibit tune-able conductivities and high ion selectivity, are ideal candidates for industrial-scale desalination or demineralization by electrodesalination.

In order to identify flux contributions the Nernst-Planck equation was utilized. This was accomplished using salt form data obtained by electrochemical impedance spectroscopy, titration, and liquid permeability studies (Table 3). As shown in Eq. (8), the Nernst-Planck equation is comprised of electroosmotic (migration), diffusion, and convection contributions. It is typically assumed that electroosmosis, or migration due to an applied electric current, is preponderant to that of diffusion and convection [41]. In Fig. 8 the ion flux for sPP1.4 and Nafion 117 was compared to that determined by the Nernst-Planck

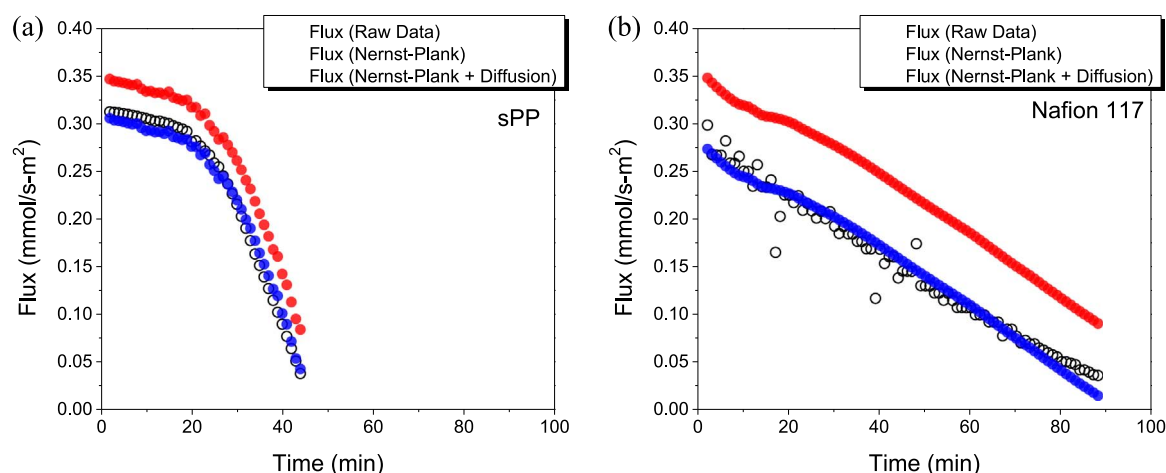


Fig. 8. Flux for sPP1.4 and Nafion 117 calculated by the change in dilute stream concentration, and modeled by the Nernst-Planck (NP) equation excluding and including back diffusion by osmosis.

equation with and without the ion diffusion (osmosis) contribution. With the consideration of diffusion by osmosis the flux determined by the Nernst-Planck equation is highly agreeable, and clearly indicates that Nafion's poor performance is largely due to poor sodium ion selectivity. This simplified model highlights the importance of ion selectivity for ED desalination and purification applications, and may prove useful in the prediction of ED performance in more exhaustive investigations.

4. Conclusions

A morphological, electrochemical, and state of water analysis was investigated for the acid and sodium forms of a series of sulfonated Diels-Alder poly(phenylene)s. sPP was found to possess a homogeneous ionic distribution, requiring greater ion exchange unit and water content to achieve comparable electrochemical performance to that of the well-ordered microstructure of Nafion 117. Despite significant differences in morphology, sPP and Nafion 117 diverge little in their relationship between proton exchange and free water. sPP displays reduced molecular and salt diffusivity, however low activation energies suggests increasing ionic domain size with temperature. Nafion 117 reveals poor performance in a working electro dialysis system, suggesting the back diffusion of ionic species into the dilute stream. sPP1.4 requires significantly less time and power to achieve desalination than the commercial material, PC-SA. This coincides with sPP's competitive electrochemical properties yet low molecular diffusivity. The Nernst-Planck equation, when accounting for back diffusion (osmosis), adequately models ED ion flux for sPP1.4 and Nafion 117.

References

- [1] T. Xu, C. Huang, Electrodialysis-based separation technologies: a critical review, *AIChE J.* 54 (2008) 3147–3159.
- [2] K.A. Mauritz, R.B. Moore, State of understanding of nafion, *Chem. Rev.* 104 (2004) 4535–4586.
- [3] S.J. Peighambaridoust, S. Rowshanzamir, M. Amjadi, Review of the proton exchange membranes for fuel cell applications, *Int. J. Hydrog. Energy* 35 (2010) 9349–9384.
- [4] B. Schwenzer, et al., Membrane development for vanadium redox flow batteries, *ChemSusChem* 4 (2011) 1388–1406.
- [5] G.M. Geise, B.D. Freeman, D.R. Paul, Sodium chloride diffusion in sulfonated polymers for membrane applications, *J. Memb. Sci.* 427 (2013) 186–196.
- [6] P. Zschocke, D. Quellmalz, Novel ion exchange membranes based on an aromatic polyethersulfone, *J. Memb. Sci.* 22 (1985) 325–332.
- [7] M. Oroujzadeh, S. Mehdipour-Ataei, M. Esfandeh, Preparation and properties of novel sulfonated poly(arylene ether ketone) random copolymers for polymer electrolyte membrane fuel cells, *Eur. Polym. J.* 49 (2013) 1673–1681.
- [8] Y.G. Jeong, et al., Synthesis and characterization of sulfonated bromo-poly(2,6-dimethyl-1,4-phenylene oxide)-co-(2,6-diphenyl-1,4-phenylene oxide) copolymer as proton exchange membrane, *Electrochim. Acta* 55 (2010) 1425–1430.
- [9] D. Chen, S. Wang, M. Xiao, Y. Meng, Synthesis and properties of novel sulfonated poly(arylene ether sulfone) ionomers for vanadium redox flow battery, *Energy Convers. Manag.* 51 (2010) 2816–2824.
- [10] C.H. Fujimoto, M.A. Hickner, C.J. Cornelius, D.A. Loy, Ionomeric poly(phenylene) prepared by diels-alder polymerization: synthesis and physical properties of a novel polyelectrolyte, *Macromolecules* 38 (2005) 5010–5016.
- [11] L. He, C.H. Fujimoto, C.J. Cornelius, D. Perahia, From solutions to membranes: structure studies of sulfonated polyphenylene ionomers, *Macromolecules* 42 (2009) 7084–7090.
- [12] R.J. Stanis, et al., Evaluation of hydrogen and methanol fuel cell performance of sulfonated diels alder poly(phenylene) membranes, *J. Power Sources* 195 (2010) 104–110.
- [13] C. Fujimoto, S. Kim, R. Stains, X. Wei, Vanadium redox flow battery efficiency and durability studies of sulfonated Diels Alder poly(phenylene)s, *Electrochem. Commun.* 20 (2012) 48–51.
- [14] U. Kumar, T. Neenan, Diels-Alder polymerization between bis(cyclopentadienones) and acetylenes. A versatile route to new highly aromatic polymers, *Macromolecules* 28 (1995) 124–130.
- [15] M. Hickner, C. Fujimoto, C. Cornelius, Transport in sulfonated poly(phenylene)s: proton conductivity, permeability, and the state of water, *Polymer (Guildf)* 47 (2006) 4238–4244.
- [16] M. Hibbs, C. Fujimoto, C. Cornelius, Synthesis and characterization of poly(phenylene)-based anion exchange membranes for alkaline fuel cells, *Macromolecules* 42 (2009) 8316–8321.
- [17] R.S. McLean, M. Doyle, B.B. Sauer, High-resolution imaging of ionic domains and crystal morphology in ionomers using AFM techniques, *Macromolecules* 33 (2000) 6541–6550.
- [18] R. Moore, C. Martin, Morphology and chemical properties of the Dow perfluorosulfonate ionomers, *Macromolecules* 22 (1989) 3594–3599.
- [19] B.P. Grady, Review and critical analysis of the morphology of random ionomers across many length scales, Wiley Intersci. (2008). <http://dx.doi.org/10.1002/pen>.
- [20] K.A. Page, F.A. Landis, A.K. Phillips, R.B. Moore, SAXS analysis of the thermal relaxation of anisotropic morphologies in oriented Nafion membranes, *Macromolecules* 39 (2006) 3939–3946.
- [21] S.A. Visser, S.L. Cooper, Analysis of small-angle x-ray scattering data for model polyurethane ionomers: evaluation of hard-sphere models, *Macromolecules* 24 (1991) 2584–2593.
- [22] H.R. Schubach, E. Nagy, B. Heise, Short range order of amorphous polymers derived by WAXS, *Colloid Polym. Sci.* 259 (1981) 789–796.
- [23] J.R. Katz, X-Ray spectroscopy of polymers and in particular those having a rubber-like extensibility, *Rubber Chem. Technol.* 9 (1936) 357–372.
- [24] G.R. Mitchell, A.H. Windle, Structure of polystyrene glasses, *Polymer (Guildf)* 25 (1984) 906–920.
- [25] C. Ayyagari, D. Bedrov, G.D. Smith, Structure of atactic polystyrene: a molecular dynamics simulation study, *Macromolecules* 33 (2000) 6194–6199.
- [26] X. Lu, W.P. Steckle, R.A. Weiss, Ionic aggregation in a block copolymer ionomer, *Macromolecules* 26 (1993) 5876–5884.
- [27] C. Zhao, et al., Block sulfonated poly(ether ether ketone)s (SPEEK) ionomers with high ion-exchange capacities for proton exchange membranes, *J. Power Sources* 162 (2006) 1003–1009.
- [28] Z. Lu, G. Polizos, D.D. Macdonald, E. Manias, State of water in perfluorosulfonate ionomer (nafion 117) proton exchange membranes, *J. Electrochem. Soc.* 155 (2008) B163–B171.
- [29] K.D. Kreuer, On the development of proton conducting polymer membranes for hydrogen and methanol fuel cells, *J. Memb. Sci.* 185 (2001) 29–39.
- [30] R.M. Hodge, G.H. Edward, G.P. Simon, Water absorption and states of water in semicrystalline poly(vinyl alcohol) films, *Polymer (Guildf)* 37 (1996) 1371–1376.
- [31] H. Yoshida, Y. Miura, Behavior of water in perfluorinated ionomer membranes containing various monovalent cations, *J. Memb. Sci.* 68 (1992) 1–10.
- [32] K. Schmidt-Rohr, Q. Chen, Parallel cylindrical water nanochannels in Nafion fuel-cell membranes, *Nat. Mater.* 7 (2008) 75–83.
- [33] F. Orfino, S. Holderoft, The morphology of nafion: are ion clusters bridged by channels or single ionic sites?, *J. New Mater. Electrochem. Syst.* 292 (2000) 287–292.
- [34] N. Carretta, V. Tricoli, F. Picchioni, Ionomeric membranes based on partially sulfonated poly(styrene): synthesis, proton conduction and methanol permeation, *J. Memb. Sci.* 166 (2000) 189–197.
- [35] G. Gebel, Structural evolution of water swollen perfluorosulfonated ionomers from dry membrane to solution, *Polymer (Guildf)* 41 (2000) 5829–5838.
- [36] M. Gil, et al., Direct synthesis of sulfonated aromatic poly(ether ether ketone) proton exchange membranes for fuel cell applications, *J. Memb. Sci.* 234 (2004) 75–81.
- [37] B. Einsla, et al., Sulfonated naphthalene dianhydride based polyimide copolymers for proton-exchange-membrane fuel cells II. Membrane properties and fuel cell performance, *J. Memb. Sci.* 255 (2005) 141–148.
- [41] F.J. Borges, H. Roux-de Balmann, R. Guardani, Investigation of the mass transfer processes during the desalination of water containing phenol and sodium chloride by electro dialysis, *J. Memb. Sci.* 325 (2008) 130–138.